Int. J. Heat Mass Transfer. Vol. 12, pp. 1465–1489. Pergamon Press 1969. Printed in Great Britain

GROWTH RATES OF FREE VAPOR BUBBLES IN LIQUIDS AT UNIFORM SUPERHEATS UNDER NORMAL AND ZERO GRAVITY CONDITIONS

L. W. FLORSCHUETZ, C. L. HENRY* and A. RASHID KHAN
Mechanical Engineering Department, Arizona State University, Tempe, Arizona

(*Received* 3 *September* 1968 *and in revised form* 16 *April* 1969)

Abstract—Extensive experimental data is presented for growth rates of vapor bubbles in water, ethanol, and isopropanol at small uniform superheats up to 4·9°C. The measured phase growth occurred in the free volume of the liquid away from solid surfaces and at a nominal pressure level of 1 atm. Uniform, essentially constant superheats were obtained by a pressure release technique. Initial observation times for most bubbles occurred at about 1 ms. Final observation times as large as 450 ms were achieved. Comparison of growth data taken at normal gravity to data taken at zero gravity, using a small drop tower, clearly show the point at which effects due to bubble translational motion become significant.

A detailed comparison is made to Scriven's exact solution for spherically symmetric, heat transfer controlled phase growth. Good agreement is obtained for the zero-g data over the entire observation time, while the agreement for the normal-g data is satisfactory up to times at which effects of the buoyant force become significant. An interpretation that the increased growth rates observed at later times is due to bubble translational effects is supported by a semi-quantitative comparison to an approximate theory due to Aleksandrov *et al.*

Previous experimental results for bubble growth under uniform, essentially constant superheat conditions and their relation to the present work are also discussed.

NOMENCLATURE

c_p, specific heat of liquid;
C, constant of proportionality defined by $U = CR$;
Ja, Jakob number, $\rho c_p \Delta T/\rho_v h_{fg}$;
h_{fg}, enthalpy of vaporization;
p^*_∞, final pressure in liquid system;
R, bubble radius;
t, time;
t_0, zero time corresponding to zero bubble radius;
t_1 and t_2, specific times defined in text prior to equations (3) and (4);
T_∞, bulk temperature of liquid;
T_s, saturation temperature corresponding to p^*_∞;
ΔT, superheat temperature difference, $(T_\infty - T_s)$;
U, bubble translational velocity;
x, dummy variable;
Z, defined in text following equation (4).
κ, thermal diffusivity of liquid;
β, bubble growth constant;
ε, defined as $(1-\rho_v/\rho)$;
ϕ, function defined following equation (2);
ρ, density of liquid;
ρ_v, density of vapor.

* Currently with AiResearch Manufacturing Co., Phoenix, Arizona.

INTRODUCTION

IT APPEARS to be fairly generally accepted that the theoretical predictions for spherically symmetric bubble growth rates controlled by heat transfer [1–3] have been adequately verified by experimental results; see, for example, references [2, 4–6]. In 1960, however, Westwater [7] pointed out that the only data available were

those of Dergarabedian [8] for water. He also noted that Dergarabedian had used unspecified size chalk dust and sand sprinkled into the superheated water to cause nucleation, so that his bubbles actually began growing on solid particles. Subsequently, Dergarabedian [9] published data for four organic liquids. He stated that the experimental procedures were the same as for his earlier work. It is not clear whether this included the use of chalk dust or sand particles. In Dergarabedian's work infra-red heating was used to uniformly raise the liquids to superheats up to 6·3°C. Re-examination of this data shows that the organic liquid data is in good agreement with Scriven's exact solution,* while the water data exhibits only fair agreement.

More recently, additional data for vapor bubbles growing in spherically symmetric temperature fields at essentially constant superheats has become available. Hooper and Abdelmessih [11] reported data for five water vapor bubbles; Hewitt and Parker [12], for nine bubbles growing in liquid nitrogen; Aleksandrov *et al.* [13], for a propane bubble in a high pressure bubble chamber; and Kosky [14] for one water vapor bubble. The uniform superheats in all of these experiments were obtained by a pressure release on the liquid system.

In [8, 9, 11 and 14] the initial observation times were about 1 msec or less. The final observation times for individual bubbles ranged from a minimum of 3 msec to a maximum of 15 msec. In [12] and [13] the earliest initial observation time was at 18 msec after the zero time. An appropriate zero time corresponding to zero bubble radius is ordinarily selected by comparison of the data to theoretical curves. Thus, in each case individual bubbles were observed only over the initial *or* the later stages of the macroscopic growth.

* Scriven [2], Birkoff *et al.* [1], and Kirkaldy [10] independently developed self-similar solutions for the problem of spherically symmetric, diffusion controlled phase growth. Here, Scriven's results are used because he presented tables of values for the integral which appears in the solution.

This paper presents extensive additional bubble growth data for bubbles growing in water, ethanol, and isopropanol under normal gravity conditions and for water and ethanol under zero gravity conditions. The bubbles grew under essentially constant superheat conditions obtained by a pressure release technique. Equivalent superheats ranged from 2·2 to 4·9°C. Initial and final observation times were from around 1 msec up to a minimum of 38 and a maximum of 140 msec for normal-g data, and from around 1 msec up to a minimum of 30 and a maximum of 450 msec for zero-g data.

The data is systematically compared to Scriven's exact solution for spherically symmetric heat transfer controlled growth. Good agreement is obtained over the entire observation intervals for the zero-g data. For the normal -g data agreement is good over the early growth but growth rates are larger than predicted during later stages of growth. This is to be expected since translational effects become significant, and these are not accounted for in Scriven's model. Semi-quantitative comparison is made to an approximate theory due to Aleksandrov *et al.* [13] which accounts for bubble translational motion. This comparison supports the interpretation that the deviation observed for normal-g data can be attributed to effects of translational motion. Comparison of normal-g and zero-g data indicates the point at which translational effects become significant. Finally, the previous work already mentioned here is discussed in more detail.

Verification of theory for uniform superheat conditions is of direct importance for application to processes such as flash vaporization and volume boiling. Furthermore, it is important that the limitations of the uniform superheat theory and its relation to experimental results be well understood, in light of many recent papers presenting data for bubble growth in surface boiling; see, for example, references [15–19]. Frequently comparison is attempted with theories similar to the uniform superheat theory but modified in some way to account for

the nonuniform temperature fields in which surface boiling bubbles actually grow.

EXPERIMENTAL APPARATUS AND PROCEDURE

The basic approach used to obtain a uniform superheat condition was to suddenly decrease the pressure on an essentially saturated liquid volume. Vapor bubble growth occurred from microscopic or nearly microscopic bubbles present in the liquid volume. Bubble histories were recorded on 16 mm film using a hi-speed Wollensak Fastex Camera.

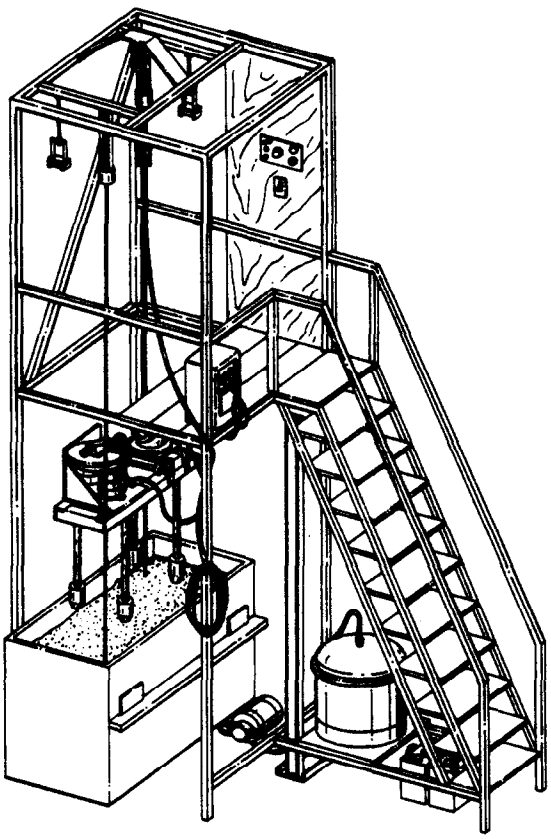

FIG. 1. Experimental facility.

Figure 1 is a general view of the experimental facility. It is similar to that used by Florschuetz and Chao to study bubble collapse [20]. The camera was mounted near one end of a steel frame. The experimental vessel was mounted on the frame opposite the camera. Tests at near zero gravity were conducted by hoisting the frame to the top of the superstructure where it was suspended from two electro-magnets. From this position it could be dropped through a distance of 8–9 feet, and then decelerated by plungers entering a box of coarse sand. For tests at normal gravity the frame was left in a stationary position near the base of the superstructure.

The cylindrical experimental vessel (Fig. 2) constructed of aluminium, was 6 in. in diameter and 10 in. high. Three Pyrex glass ports each 3 in. in diameter were provided for photography, back lighting, and viewing. A gas plate was mounted at the base of the vessel for heating of

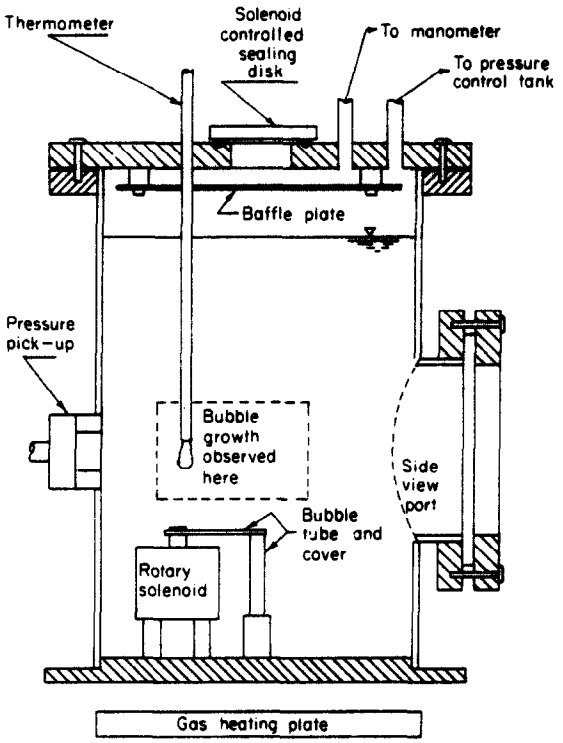

FIG. 2. Experimental vessel. The side view port is shown. Identical front and rear ports for photography and lighting are not shown.

the test liquid. The vessel was originally designed for studies of vapor bubble condensation rates. Therefore, a small vertical glass tube with a rotary solenoid controlled cover over its upper end was positioned near the bottom of the vessel in order to introduce a controlled size vapor bubble at the desired instant. This mechanism was present in the vessel during the bubble growth tests but was not necessary for controlled introduction of bubble nuclei. In these tests microscopic or nearly microscopic bubbles originating from natural nucleation sites were present in the field of view at the instant of pressure release and provided the nuclei from which the phase growth occurred. A Dynisco Model PT85-5, 0–5 psig pressure pickup was flush mounted on the side of the vessel.

In preparation for a test run the liquid was boiled for at least 30 min at atmospheric pressure. The heating rate was then reduced while a one inch opening at the top of the vessel was sealed by a metal disk using a Viton O-ring. The sealing disk was arranged in such a way that it could be suddenly released by activating a solenoid. The vessel was pressurized to a level 10–25 cm Hg above atmospheric by a large pressure control tank. In about 5 minutes a saturated boiling condition was again obtained which was continued at a slow, steady rate for another five minutes. A cooling period of about 30s–1 min was then allowed during which the boiling essentially subsided. The bulk temperature dropped from about 0·1 to 0·3°C depending on the cooling period. At this time the liquid temperature was recorded from a mercury-in-glass thermometer. The pressure was read from a 79 in. large bore Meriam manometer filled with No. 3 manometer fluid. A spot lamp was switched on to provide back lighting for photography. The camera switch was closed. The camera accelerated to a rate of at least 1 200 frames/s. A relay caused the solenoid controlled sealing disk to release, suddenly reducing the system pressure. This procedure was used for all test runs at normal gravity. A similar procedure was used for runs at zero gravity, except that during the acceleration period of the camera a relay caused the release of the frame from the supporting electromagnets. The solenoid control on the sealing disk was then activated manually about half way through the drop. The procedure is summarized in Fig. 3. When desired, the system pressure variation during a run was monitored with the pressure pickup.

EXPERIMENTAL RESULTS

For successful runs a number of bubbles growing in the volume of the liquid were visible on the film. However, only those bubbles which were in sharp focus and provided a good contrast outline on the film were selected for data reduction. Furthermore, only bubbles reasonably isolated from their neighbors wer selected. The bubble populations were such that selected bubbles usually had only one or two neighbors

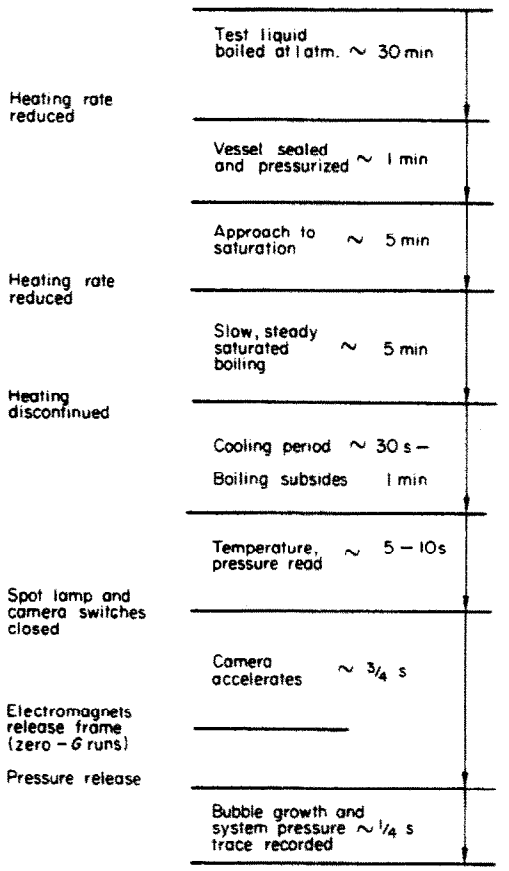

FIG. 3. Summary of test run procedure.

as close as a diameter and most were much more isolated.

Test runs at normal gravity were made using demineralized, once distilled water, reagent grade ethanol, and reagent grade isopropanol. Twenty runs resulted in usable data for at least one bubble and several provided data for two bubbles. The runs which did not result in usable data were those in which longer cooling periods were allowed. Fewer bubble nuclei were present in these cases, thus reducing the probability of one being present in the field of view and in proper focus. Six runs were made at near zero gravity conditions, using water and ethanol as test liquids. All runs except one resulted in usable data for at least one bubble since the cooling period was judged from previous experience in order to insure a sufficiently high bubble nuclei population.

Bubble sizes were measured by hand after magnification of the film on a microfilm reader. The scale factor was determined from a scale of known dimensions mounted in the experimental vessel (not shown in Fig. 2) which was always present in the field of view. When bubbles departed from a spherical shape they appeared, in cross-section, to approximate oblate spheroids. An equivalent bubble radius was determined by arithmetically averaging the major and minor axes. With few exceptions, aspect ratios for zero-g runs never departed significantly from unity. Aspect ratios for normal-g runs ranged from unity to about 3, but the larger values only occurred when bubbles were followed to equivalent radii up to about 0·3 cm. Departure from sphericity began at radii of 0·05 cm for alcohol bubbles and at 0·1 cm for water bubbles. A more appropriate equivalent radius could, perhaps, have been calculated based on the volume of an oblate spheroid. However, the arithmetic mean radius falls at most only 5 per cent below the oblate spheroid value for the range of aspect ratios involved. The absolute uncertainty associated with the equivalent bubble radii is estimated to be about $\pm 0{\cdot}005$ cm.

Relative times were determined from timing marks on the edge of the film produced by a timing light located inside the camera. The uncertainty on the time-scale is judged to be negligible compared to the uncertainty associated with selecting a zero time.

For illustrative purposes, magnified bubble tracings for Bubble 7 (normal-g) and Bubble 24 (zero-g) are shown in Figs. 4 and 5. The contrast between these bubbles is evident. Bubble 7 had the larger rate of vertical displacement and departed from sphericity due to the translational motion. Bubble 24 had a small rate of displacement and remained essentially spherical. Translational velocities were measured, but are not reported in detail because they represent values

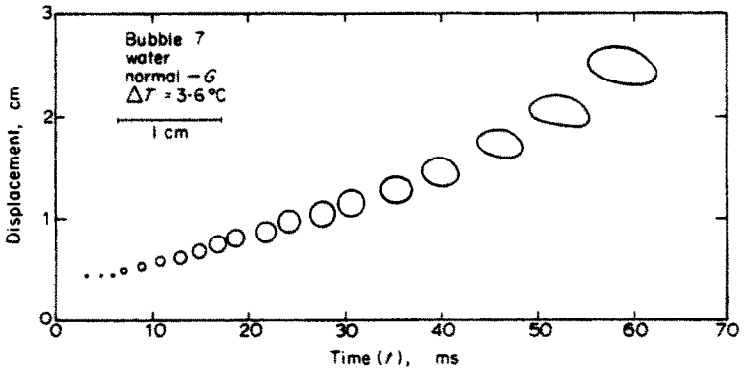

FIG. 4. Illustration of bubble growth at normal gravity.

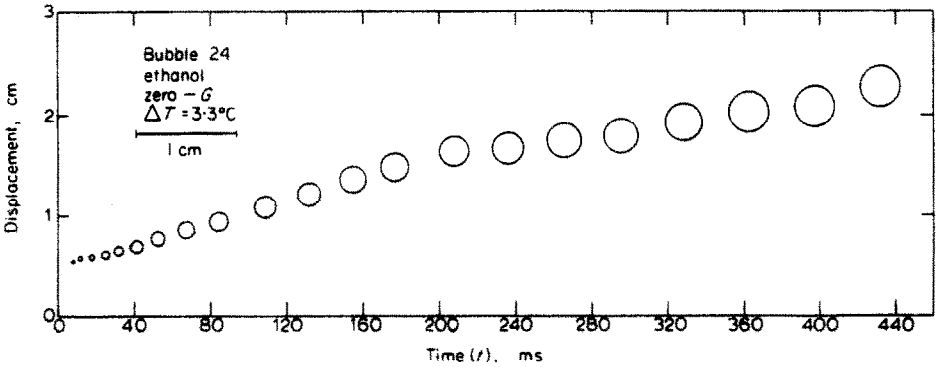

FIG. 5. Illustration of bubble growth at zero gravity.

with respect to a reference frame fixed to the vessel. Their use as relative velocities to the liquid would be in error. There was some relative motion between the liquid and the vessel since during phase growth the fluid expanded into the free volume at the top of the vessel. Thus, bubble velocities relative to the liquid were less than those relative to the vessel, but precisely how much less is not known. Measured values relative to the vessel ranged from 0–20 cm/s for zero-g runs and from 0–40 cm/s for normal-g runs. The finite velocities during zero-g runs were attributed mainly to the upward motion of the liquid as it expanded into the free volume. The velocities for normal-g runs were due to the upward liquid motion plus the velocity relative to the liquid caused by the buoyant force.

Tabular data for Bubbles 7 and 24 is presented in Table 1.* The Table displays the values of the magnified major and minor diameters (D1 and D2) and the equivalent radii calculated from $R = 0{\cdot}25$ (D1 + D2) (Scale factor). The times indicated are measured from an arbitrary zero time. Selected zero times (t_0) indicated in the Table were used for comparison of data to theory. The method of zero time selection is illustrated in the next section. The reported superheat temperature differences represent the difference between the directly measured bulk temperature, T_∞, and the saturation temperature, T_s, corresponding to the final system pressure, p^*_∞.

* Similar tabular data for all runs reported herein is available from the authors.

Table 1. *Tabular data for bubble* 7 (*water, normal -g*) *and bubble* 24 (*ethanol, zero -g*)

Frame	D1 (cm)	D2 (cm)	R (cm)	Time (ms)	$R/2\beta\kappa^{\frac{1}{2}}$
Bubble 7, ΔT = 3·61°C, t_0 = 6·5 ms					
5	0·075	0·050	0·0119	3·19	0·0142
7	0·075	0·050	0·0119	4·47	0·0142
9	0·075	0·075	0·0143	5·75	0·0170
11	0·150	0·150	0·0286	7·02	0·0340
14	0·200	0·200	0·0381	8·94	0·0454
17	0·275	0·275	0·0524	10.86	0·0624
20	0·350	0·325	0·0643	12·77	0·0765
23	0·375	0·350	0·0691	14·69	0·0822
26	0·450	0·425	0·0833	16·60	0·0992
29	0·475	0·450	0·0881	18·52	0·1049
34	0·525	0·525	0·1000	21·71	0·1191
38	0·600	0·550	0·1095	24·27	0·1304
43	0·675	0·600	0·1214	27·46	0·1446
48	0·750	0·650	0·1333	30·65	0·1587
55	0·825	0·700	0·1453	35·12	0·1729
62	0·950	0·750	0·1619	39·59	0·1928
72	1·225	0·750	0·1881	45·98	0·2240
82	1·600	0·775	0·2262	52·36	0·2693
92	1·900	0·975	0·2738	58·75	0·3260
Bubble 24, ΔT = 3·26°C, t_0 = 7 ms					
8	0·100	0·100	0·0190	6·64	0·0594
11	0·100	0·100	0·0190	9·12	0·0594
14	0·125	0·100	0·0214	11·62	0·0668
18	0·150	0·150	0·0285	14·95	0·0891
22	0·175	0·175	0·0332	18·27	0·1039
26	0·200	0·175	0·0356	21·60	0·1113
30	0·225	0·225	0·0427	24·90	0·1336
34	0·250	0·250	0·0475	28·25	0·1484
38	0·275	0·275	0·0522	31·55	0·1633
42	0·275	0·275	0·0522	34·90	0·1633
46	0·300	0·275	0·0546	38·20	0·1707
50	0·300	0·300	0·0570	41·55	0·1781
54	0·325	0·325	0·0617	44·80	0·1930
58	0·350	0·325	0·0641	48·20	0·2004
63	0·350	0·350	0·0665	52·30	0·2078
68	0·375	0·375	0·0712	56·50	0·2227
74	0·400	0·400	0·0760	61·50	0·2375
81	0·425	0·425	0·0807	67·25	0·2523
88	0·450	0·450	0·0855	73·10	0·2672
95	0·450	0·450	0·0855	78·80	0·2672
103	0·475	0·475	0·0902	85·15	0·2820
113	0·525	0·500	0·0974	93·08	0·3043
123	0·525	0·525	0·0997	100·85	0·3117
133	0·550	0·525	0·1021	108·62	0·3191
143	0·575	0·550	0·1069	116·69	0·3340
153	0·600	0·550	0·1092	124·46	0·3414
163	0·625	0·600	0·1164	132·23	0·3637
173	0·650	0·625	0·1211	140·00	0·3785
183	0·675	0·625	0·1235	147·57	0·3859
193	0·675	0·625	0·1235	155·14	0·3859
203	0·675	0·675	0·1282	162·71	0·4008
213	0·725	0·700	0·1354	170·11	0·4230
223	0·725	0·700	0·1354	177·51	0·4230
233	0·750	0·725	0·1401	184·91	0·4379
248	0·750	0·750	0·1425	196·31	0·4453
263	0·750	0·750	0·1425	208·41	0·4453
279	0·775	0·750	0·1449	220·51	0·4527
300	0·825	0·775	0·1520	236·41	0·4750
320	0·825	0·825	0·1567	251·23	0·4898
340	0·850	0·850	0·1615	266·05	0·5047
360	0·875	0·875	0·1662	280·87	0·5195
380	0·900	0·900	0·1710	295·69	0·5344
400	0·925	0·925	0·1757	310·51	0·5492
425	0·975	0·950	0·1829	328·21	0·5715
450	1·025	0·950	0·1876	345·91	0·5863
475	1·025	1·025	0·1947	363·61	0·6086
500	1·050	1·025	0·1971	381·31	0·6160
525	1·125	1·025	0·2042	398·31	0·6383
550	1·050	1·050	0·1995	415·31	0·6234
575	1·075	1·075	0·2042	432·62	0·6383
600	1·100	1·100	0·2090	450·81	0·6531

The precision total immersion thermometers used, graduated to 0·1°C and 0·2°C, were certified by the manufacturer to be accurate to ± one scale division. Each thermometer was also checked at the steam point using condensing vapor prior to its use in experimental runs. Stem corrections (minor) were made when necessary.

A check using two precision thermometers calibrated against each other showed that at the end of the cooling period the temperature at the center of the liquid volume differed by less than 0·1°C from that at the outermost possible location of a selected vapor bubble. Checks using radiation shields showed that there was no measurable local heating of the liquid due to radiation from the spot lamp. An effect on thermometer reading due to direct radiation exchange between the lamp and the thermometer bulb noted when using the alcohols was precluded by delaying switching on of the lamp until just after the temperature reading was made. Considering the precautions taken, the overall uncertainty of the bulk liquid temperature values was less than ±0·2°C.

Figure 6 shows an example of a system pressure trace. The system pressure does not drop

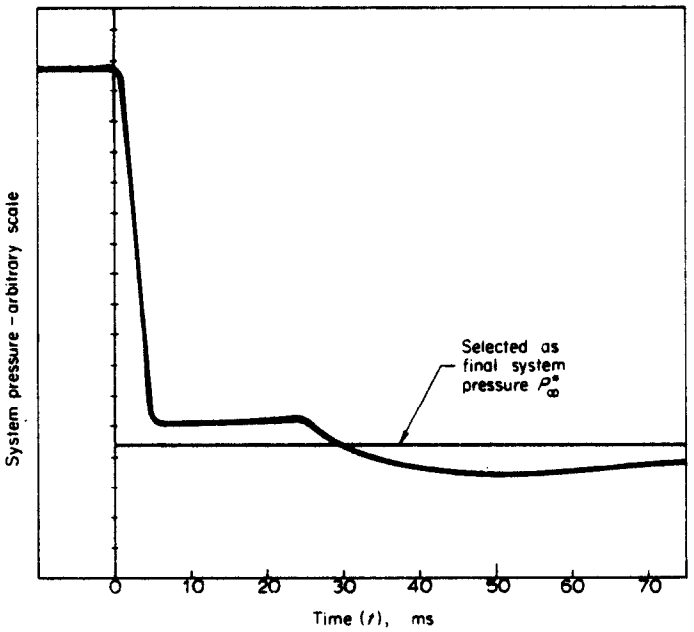

FIG. 6. Illustration of system pressure variation and selection of final system pressure.

immediately to atmospheric because of the expansion of the fluid into the free volume. However, in 5 ms it has dropped to a value somewhat greater than atmospheric and remains essentially constant thereafter for at least 80 ms. Subsequently, the expanding fluid fills the vessel and the pressure momentarily rises (not shown on Fig. 6) until enough fluid is expelled to equalize the system pressure with atmospheric. Bubble growth was measured during the period before the fluid filled the free volume, unless measurement had to be terminated earlier because of interaction with other bubbles or movement of the bubble of interest from the field of view. For zero-g runs the pressure remained essentially constant for longer periods before the fluid filled the free volume because the overall expansion rate was less than for normal-g runs. Because of this, and also because bubbles tended to remain in the field of view for longer periods, some longer observation times were obtained for zero-g runs.

Figure 6 illustrates how the final system pressure was selected in order to evaluate the equivalent superheat. The theoretical model to which the data is later compared likewise assumes a step change to a constant value. Justification for this method of evaluation, which ignores the 5 msec pressure release time and the subsequent small deviation from a constant value, is provided in the next section. Variation of p_∞^* from the selected constant value was such that variation of the pressure difference was about ± 5 per cent for water and less than ± 5 per cent for the alcohols. In all cases the variation was less than ± 10 per cent. In cases where a pressure trace was not obtained, equivalent superheat values were determined using measured values from other identical runs where pressure traces were obtained. For the same initial conditions, values obtained for the equivalent superheat were reproducible to within ± 3 per cent.

An overall assessment of the experimental uncertainties and their affect on the comparison to theory is delayed to the end of the next section.

COMPARISON TO SCRIVEN'S THEORETICAL RESULTS

Scriven's theoretical result predicts a bubble radius growing according to

$$R = 2\beta(\kappa t)^{\frac{1}{2}} \tag{1}$$

The growth constant, β, is given by

$$\phi(\varepsilon, \beta) = Ja, \tag{2}$$

where

$$\phi(\varepsilon, \beta) = 2\beta^3 \exp(\beta^2 + 2\varepsilon\beta^2) \int_{\beta}^{\infty} x^{-2} \exp(-x^2 - 2\varepsilon\beta^3 x^{-1})\, dx.$$

This integral cannot be evaluated in closed form, but Scriven [2] has presented tabular values. For cases of interest here ε may be taken as unity.* This result is an exact solution for a model which assumes an infinite body of liquid initially at a uniform saturation temperature. The pressure on the system is instantaneously reduced. Spherically symmetric vapor bubble growth from a nucleus of zero size occurs at a rate governed by the rate of heat transfer from the liquid to the bubble interface which supplies the enthalpy of vaporization for the liquid at the interface. The model neglects liquid inertia effects so that the interface temperature may be imagined to instantaneously drop to a saturation value corresponding to the reduced system pressure and remain constant at that value. Previous theoretical results [3, 22–24] show that for the range of superheats covered in this investigation the neglect of liquid inertia effects is justified. More recently, a detailed study by Al-Jubouri [21] has also verified this assumption, e.g., for a water vapor bubble at one atmosphere, and $\Delta T = 5°C$, the theoretical bubble radius based on a model which includes both liquid inertia and heat transfer effects is within 10 per cent of that predicted by the heat transfer model after only 0·06 ms.

All data was plotted as $R/2\beta\kappa^{\frac{1}{2}}$ vs. t, with β evaluated from equation (2). On such a plot, equation (1) results in a single theoretical curve for comparison to the data. Selection of an appropriate zero time was made on a Cartesian plot and is illustrated for Bubbles 7 and 24 in Figs. 7 and 8. The theoretical curve was shifted along the time axis until the best agreement with the data was obtained. Note that these bubbles had initial radii of 0·012 cm and 0·019 cm, respectively (Table 1). In all cases similar to these, where initial bubble sizes were such that they could be detected on the films before growth began, the initial radii had similar values. In other cases the initial sizes were too small to be detected on the films and growth had already just begun before the first measurement could be made. For Bubble 7 (normal-g) the data begins to depart from the theory at about 35 ms. This is attributed to effects of bubble translation relative to the liquid which become significant under normal-g conditions as the bubble size increases.

Using the approach just illustrated for zero time selection, all of the data is compared to equations (1) and (2) on log plots. The comparison for normal-g data is made in Fig. 9 for water, Fig. 10 for ethanol, and Fig. 11 for isopropanol. The comparison for zero-g is made in Fig. 12 for water and in Fig. 13 for ethanol. Bubbles denoted by identical numbers were from the same test run and are distinguished by a letter suffix. The agreement appears to be quite satisfactory. The result for Bubble 24 (Fig. 13b) is particularly striking since the observation time runs from 1 to 450 ms while the radius increases over tenfold. There is a consistent tendency for the normal-g bubbles to exhibit increased growth rates starting at times between 30 and 50 ms. A similar behavior is not evident in the case of the zero-g bubbles. It therefore seems reasonable to conclude that this effect reflects the presence of the buoyant force at normal-g, which in turn causes translation of

* An excellent approximation for the range of β's covered in the present experiments is simply to take $\phi(1, \beta) \simeq \beta$, and therefore $\beta \simeq Ja$.

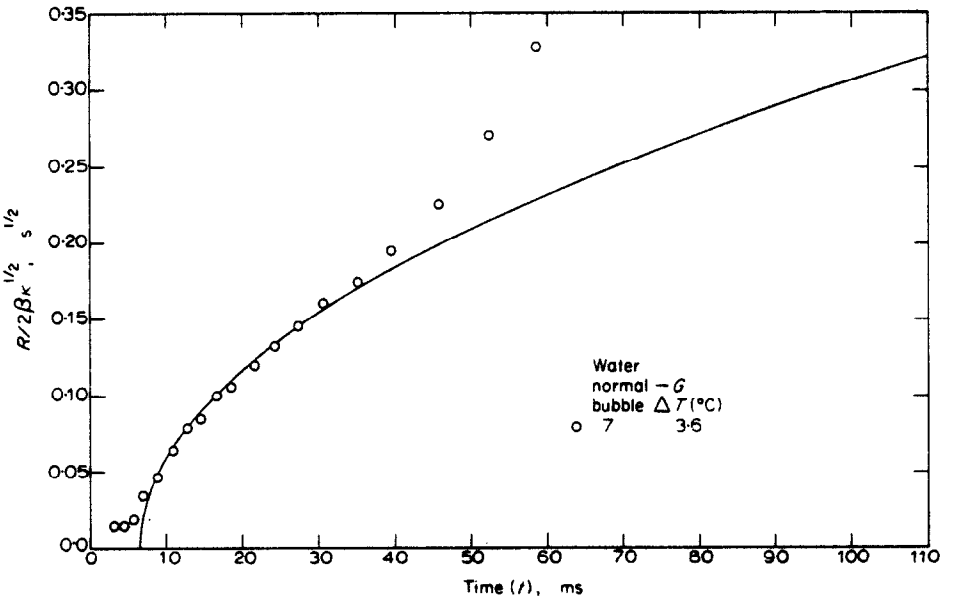

FIG. 7. Example of selection of zero time for normal gravity data.

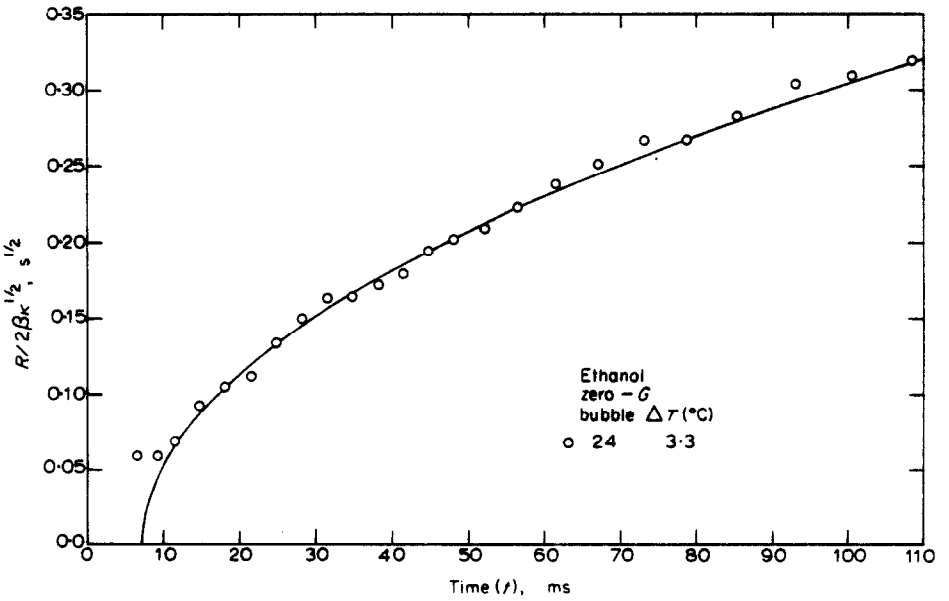

FIG. 8. Example of selection of zero time for zero gravity data.

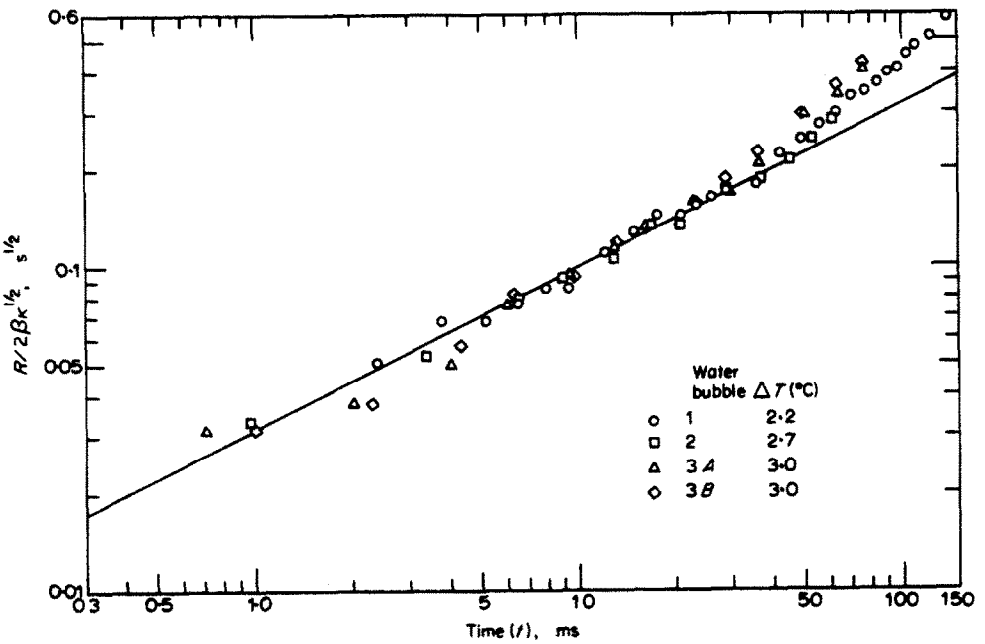

FIG. 9(a).

FIG. 9(a), (b), (c). Comparison of present water data for normal gravity to Scriven's theoretical result.

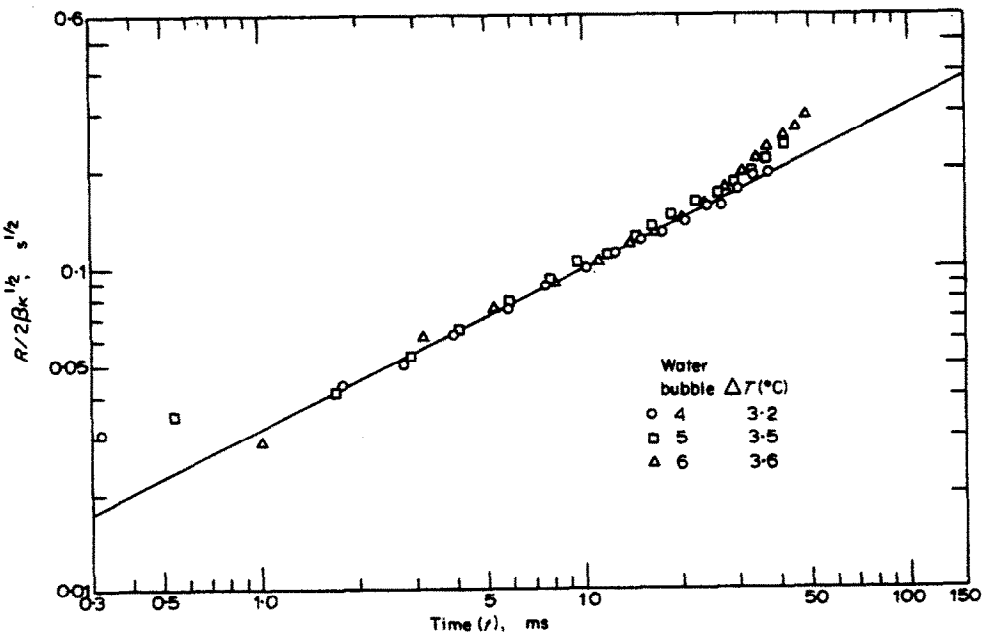

FIG. 9 (b)

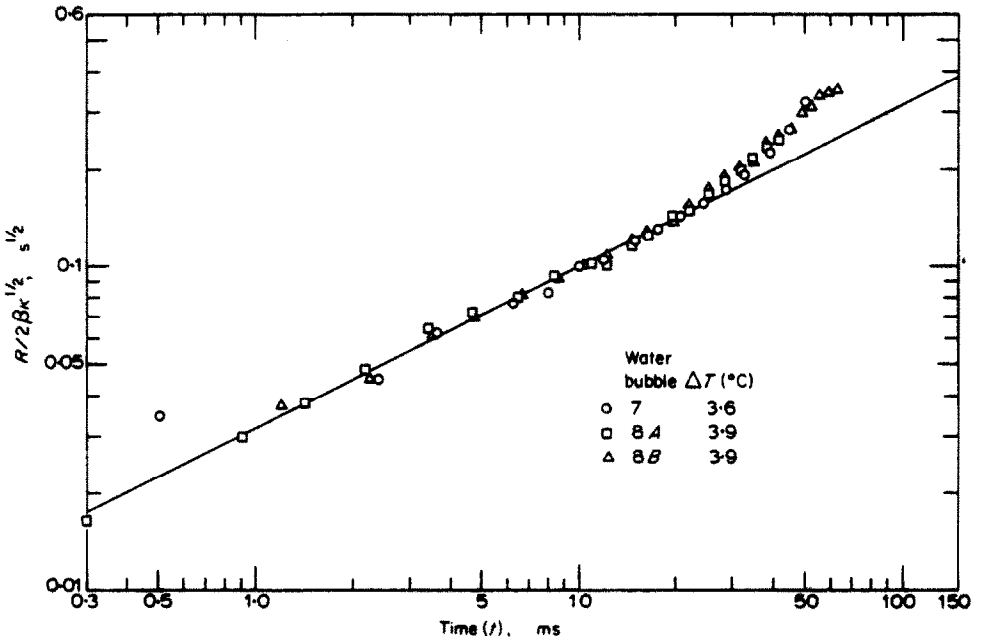

FIG. 9 (c)

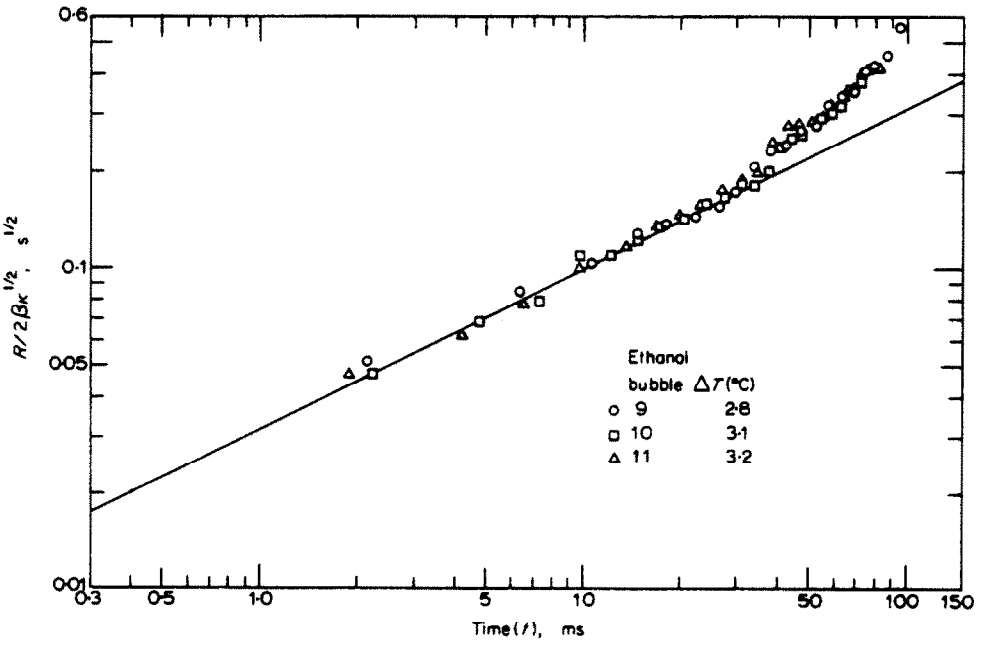

FIG. 10(a).

FIG. 10(a), (b), (c). Comparison of present ethanol data for normal gravity to Scriven's theoretical result.

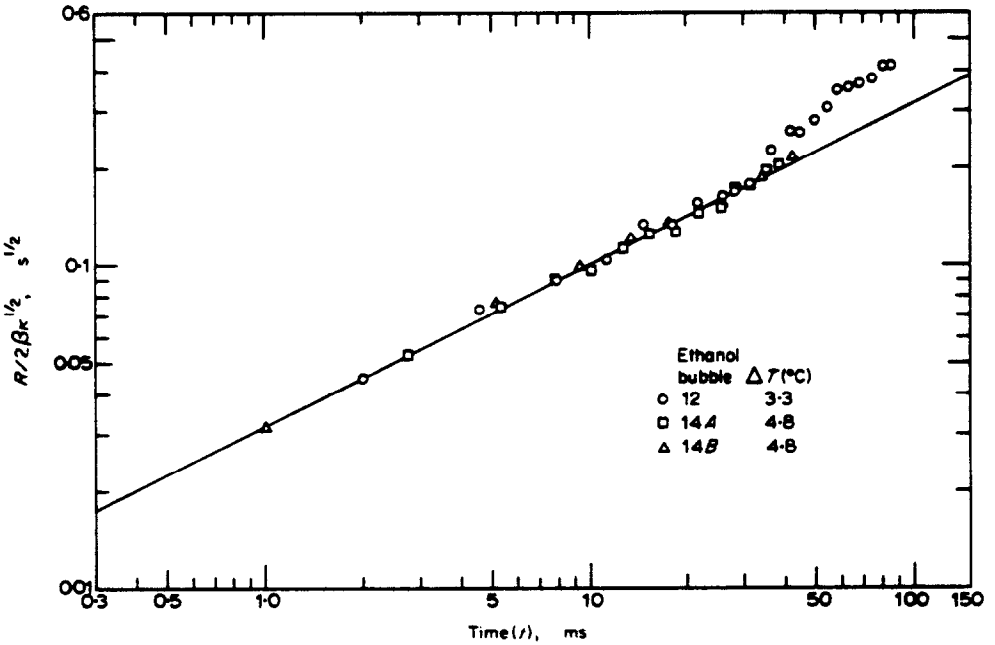

FIG. 10(b)

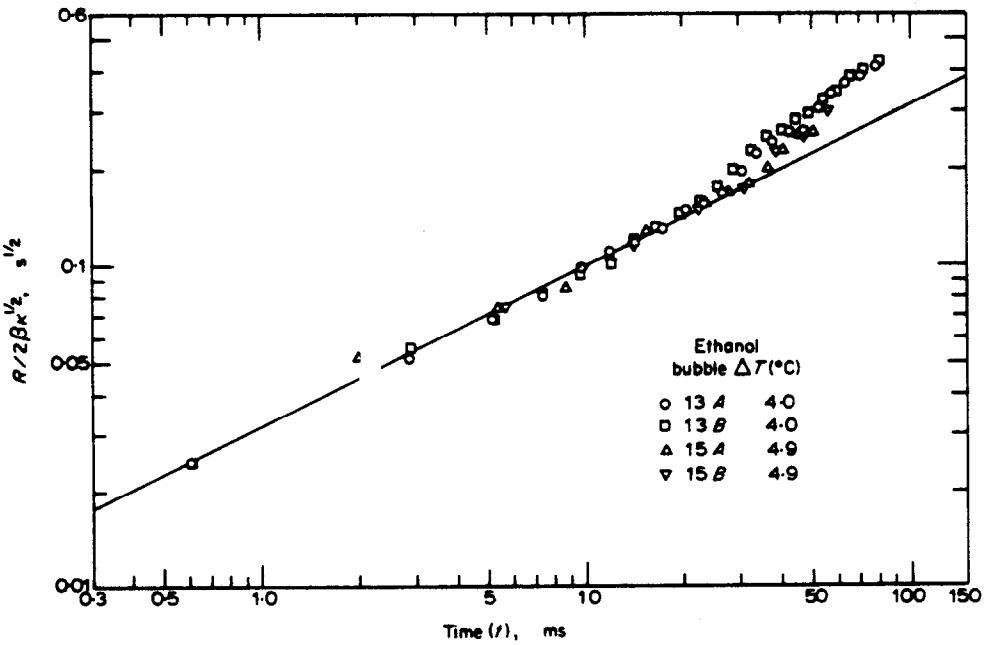

FIG. 10(c)

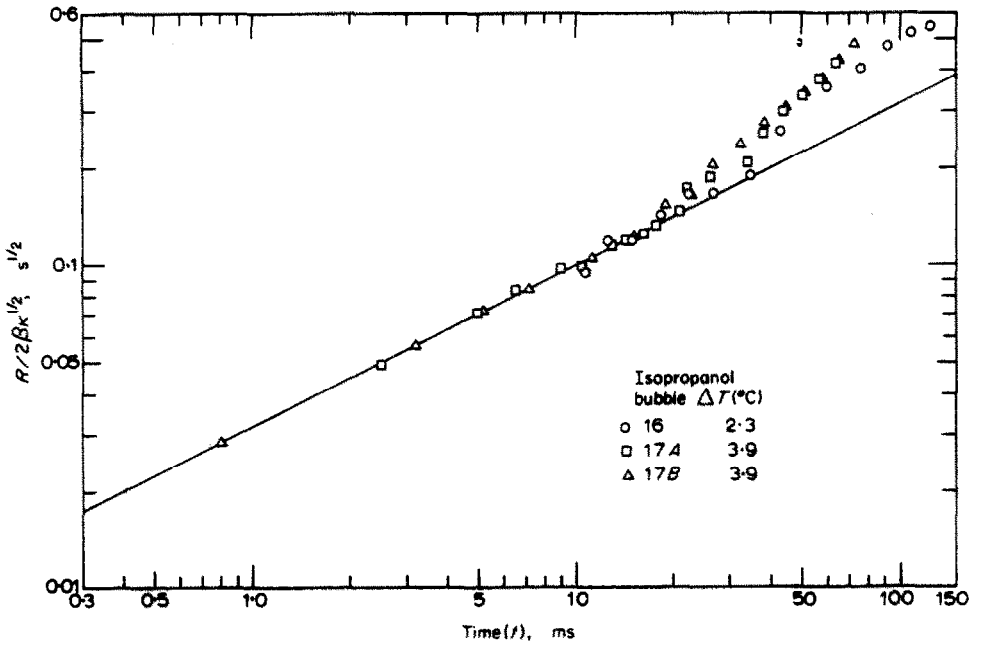

FIG. 11(a)

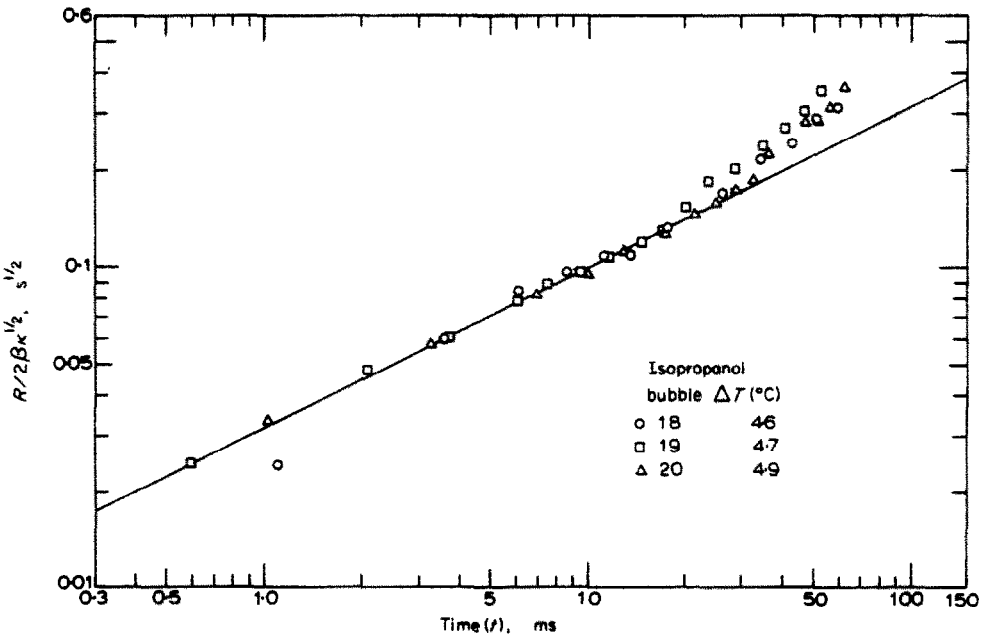

FIG. 11(b)

FIG. 11(a), (b). Comparison of present isopropanol data for normal gravity to Scriven's theoretical result.

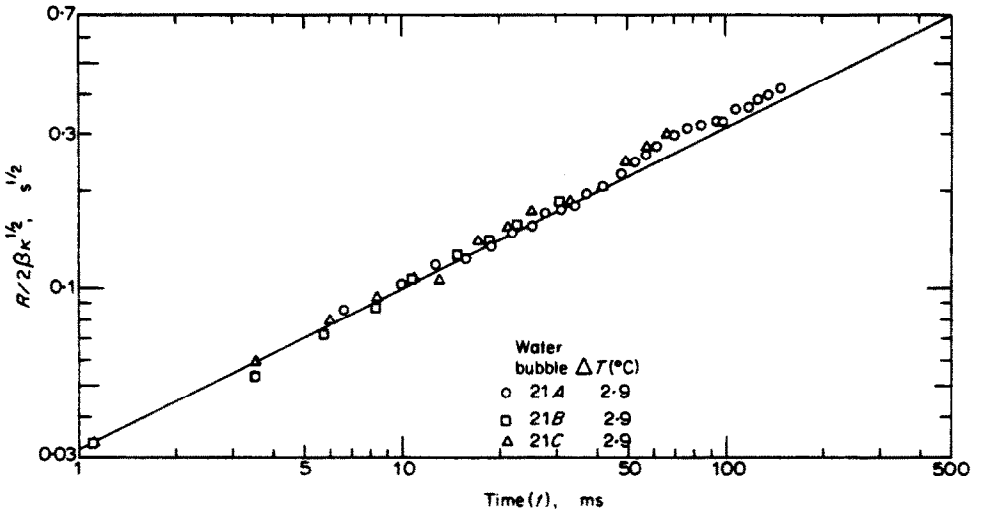

FIG. 12(a)

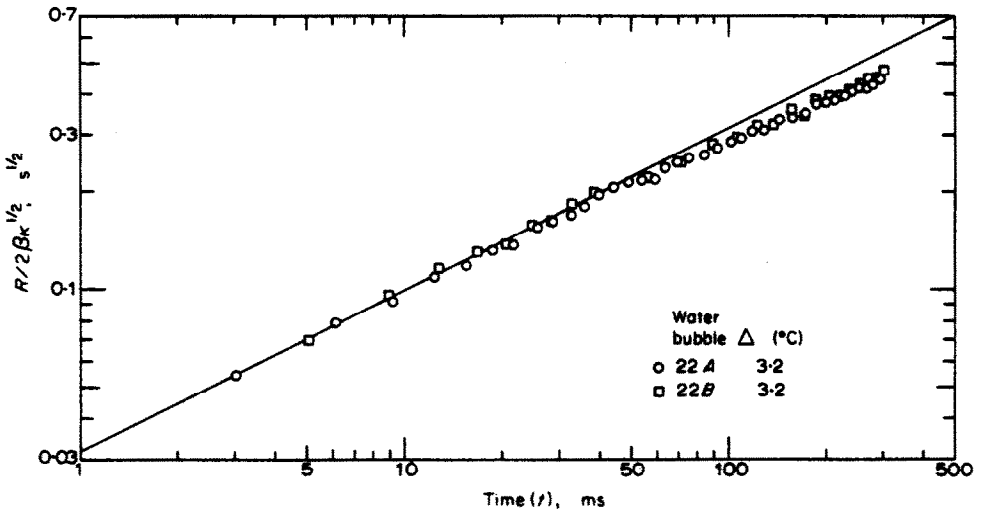

FIG. 12(b)

FIG. 12(a), (b). Comparison of present water data for zero gravity to Scriven's theoretical result.

the bubbles and a departure from sphericity. Anticipating any suggestion that larger equivalent radii may result because of the arithmetic averaging technique used when the bubble shapes departed from sphericity, and therefore do not truly reflect larger bubble volumes due to increased growth rates, it is only necessary to reiterate that the arithmetic average actually results in a slightly smaller equivalent radius than one based on the true volume of an oblate spheroid.

Before turning to consideration of an approximate theoretical analysis which includes bubble translational effects, one further point should be mentioned. The system pressure characteristically showed a small additional decrease after about 30 ms (Fig. 6). It is conceivable that the increased growth rates could have been caused

by this effect, although if this were the case one would expect a similar behavior of the zero-g data. To further check this point and also the effect of the 5 ms pressure release time, the analysis described below was performed.

Using a model like Scriven's, except considering a plane interface rather than a spherical one, simple closed form solutions for phase growth rates corresponding to simple system pressure variations can be easily obtained. Since for conditions of interest here, liquid inertia effects can be safely neglected [21], the saturation temperature, T_s, may be assumed to follow the system pressure instantaneously. Figure 14 shows three variations of T_s; a step change, and cases A and B. The latter two both represent a linear drop of T_s from $t = 0$ to t_1 ($= 5$ ms), a constant value from t_1 to t_2 ($=30$ ms) where a

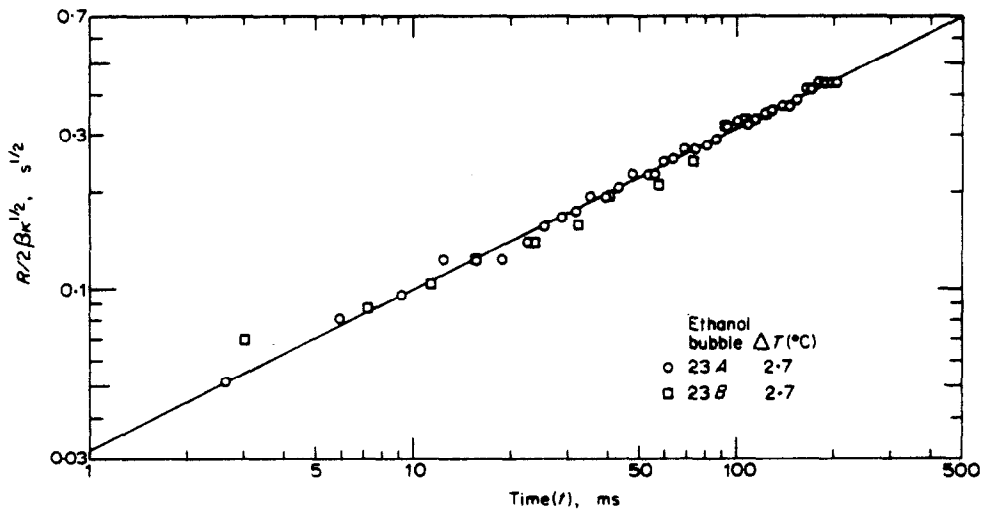

FIG. 13(a)

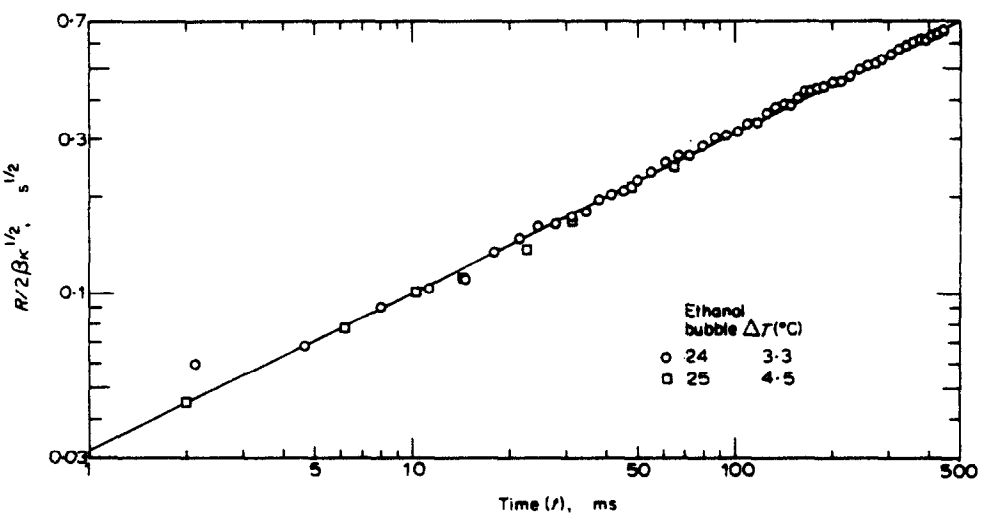

FIG. 13(b)

FIG. 13(a), (b). Comparison of present ethanol data for zero gravity to Scriven's theoretical result.

small step decrease occurs, after which T_s remains constant. These two cases more closely idealize the type of variation shown in Fig. 6 than does the step change. The plane interface model leads to the following results. For the step change,

$$R/2Ja(\kappa/\pi)^{\frac{1}{2}} = t^{\frac{1}{2}}, t > 0. \quad (3)$$

For cases A and/or B,

$$R/2Ja(\kappa/\pi)^{\frac{1}{2}} = \begin{cases} \dfrac{2(1-Z)t^{\frac{1}{2}}}{3t_1}, & 0 < t < t_1 \\ \dfrac{2(1-Z)}{3t_1}[t^{\frac{1}{2}} - (t-t_1)^{\frac{1}{2}}], & t_1 < t < t_2 \\ \dfrac{2(1-Z)}{3t_1}[t^{\frac{1}{2}} - (t-t_1)^{\frac{1}{2}}] + 2Z(t-t_2)^{\frac{1}{2}}, & t > t_2 \end{cases} \quad (4)$$

Here Z represents the fractional difference between the step change value of ΔT and the constant regions of cases A and B. In Fig. 14, $Z = 0{\cdot}05$ for case A, and $0{\cdot}10$ for case B. The solutions represented by equations (3) and (4) are shown in graphical form in Fig. 15.

Suppose that cases A and B are treated as experimental results and are to be compared to the step change case. Shifting the step change curve to the right along the time axis, selecting $t_0 = 3$ ms for case A and $t_0 = 4$ ms for case B, reasonable agreement is obtained. A comparison made on a log plot using the adjusted zero times for cases A and B is shown in Fig. 16. This analysis makes it clear that direct comparison of the data to a model based on a step change is a valid procedure, since the results are not very sensitive to these small deviations of system pressure (and, hence, saturation temperature) from the selected constant value. It is emphasized that a small step change at $t_2 = 30$ ms is more

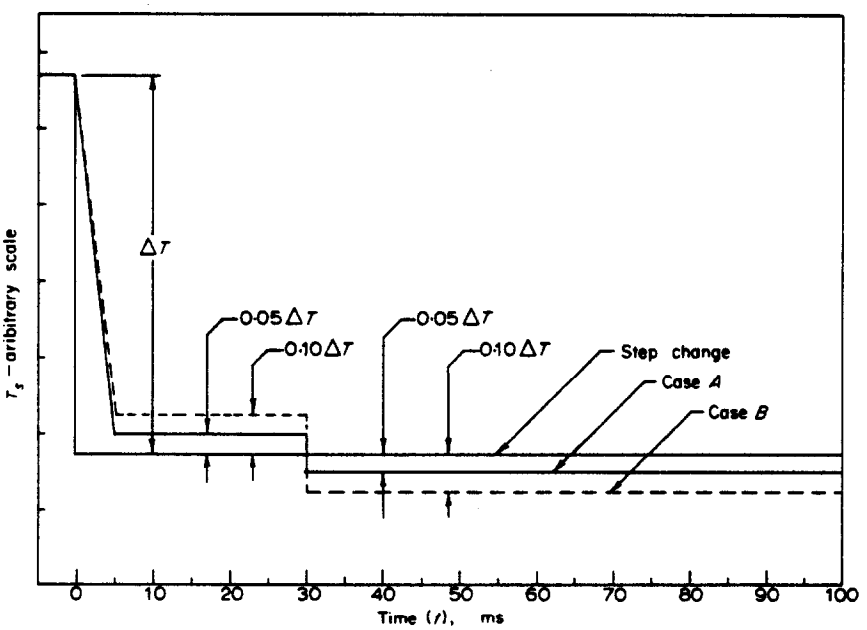

FIG. 14. Idealization of the saturation temperature variation during bubble growth.

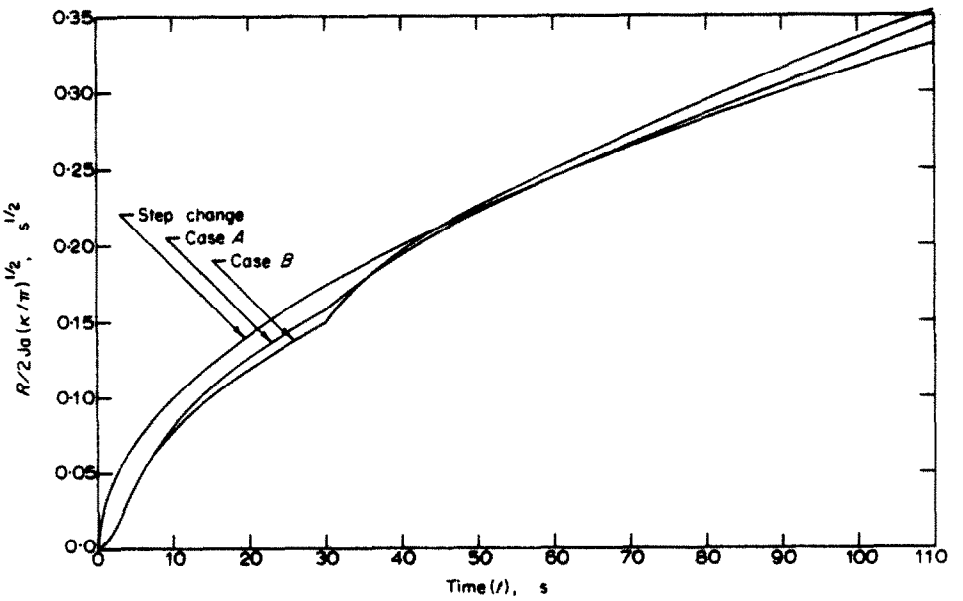

FIG. 15. Corresponding (see Fig. 14) bubble growth curves using the plane interface model.

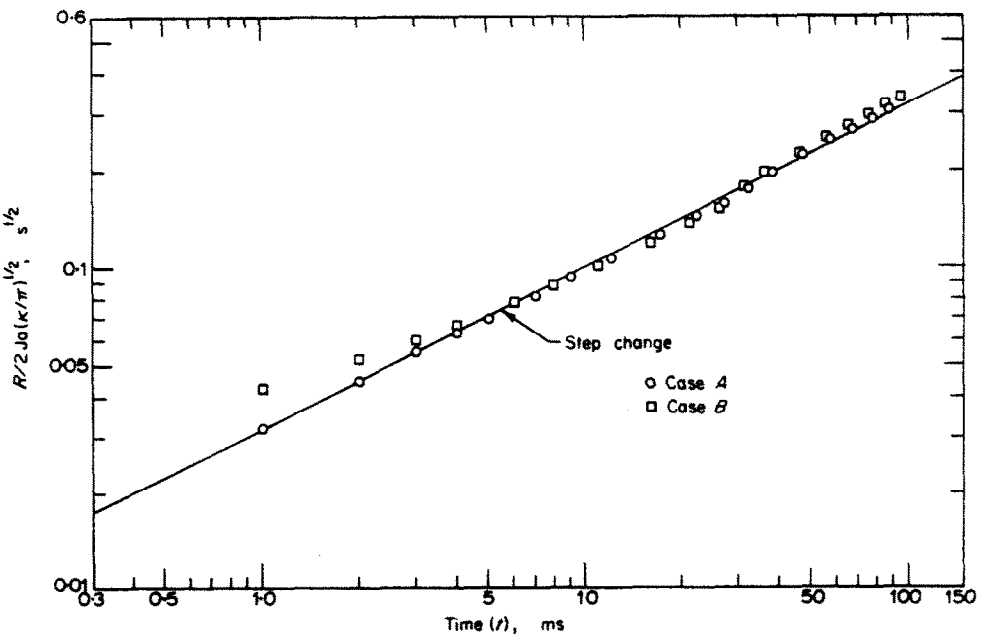

FIG. 16. Comparison of theoretical predictions using plane interface model after appropriate selection of zero time.

severe than the actual variations observed, and that the magnitude of the variation was usually ± 5 per cent or less. However, the analysis shows that even for a variation of ± 10 per cent the the effect is not extremely severe. In some cases, such as Fig. 6, the observed variation was between ± 5 and ± 10 per cent.

It is clear that the largest uncertainty in experimental evaluation of $R/2\beta\kappa^{\frac{1}{2}}$ results from the uncertainty in the value of ΔT used to calculate the Jakob number. As just demonstrated, the small variation in the value of T_s is mostly compensated for by the procedure in selecting a zero time. For most cases the percentage uncertainty in ΔT due to the uncertainty in T_∞ is within ± 10 per cent, the largest values applying for the smallest superheats. Only for the first several data points will the percentage uncertainty in the values of R be comparable to or larger than this. It is noted that most of the data points fall within ± 10 per cent of Scriven's theoretical prediction, except for the deviation of the normal-g data attributed to translational effects and some of the data points for the initial stages of growth.

EFFECT OF TRANSLATIONAL MOTION

Further justification for the interpretation that the increased growth rates observed for the normal-g data can be attributed to augmented heat transfer to the bubble interface due to translational motion can be obtained by making a semi-quantitative comparison to theoretical results based on an approximate theory presented by Aleksandrov *et al.* [13]. A detailed quantitative comparison is not made for two reasons. (1) The theory [13] assumes that the bubble maintains a spherical shape while the present data indicate that possibly significant departure from sphericity begins roughly at the same time that the increased growth rates are observed. As previously noted aspect ratios corresponding to the last data points sometimes reach values as high as three. (2) Also, for reasons already noted, the bubble translational velocities, U, relative to the liquid are not accurately known. Use of the theory requires knowledge of the functional relation between U and R for the individual bubble.

The theory is based on appropriately combining results for a stationary growing bubble and for a constant volume translating bubble. Justification for the appropriate way of combining these cases is given in [13] and will not be repeated here. The approximate result given by Aleksandrov *et al.* is

$$\frac{dR}{dt} = \frac{k\Delta T}{\rho_v h_{fg}} \left(\frac{3}{\pi\kappa t} + \frac{2U}{3\pi\kappa R} \right)^{\frac{1}{2}}. \tag{5}$$

For $U = 0$ this reduces to the Plesset–Zwick approximation [3].

In general, for $U = U(R)$ the equation is nonlinear in R. Since this function is not accurately known, we choose here to approximate it by a linear function $U = CR$ where C is a constant of proportionality. This choice certainly has the right qualitative features and conveniently renders equation (5) linear, and subject to integration using standard integral tables. The result is

$$R/2Ja(3\kappa/\pi)^{\frac{1}{2}} = \tfrac{1}{6}[t(2Ct + 9)]^{\frac{1}{2}} + (9/8C)^{\frac{1}{2}} \ln \{\tfrac{1}{3}[(2Ct + 9)^{\frac{1}{2}} + (2Ct)^{\frac{1}{2}}]\}. \tag{6}$$

In the limit as $C \to 0$ this becomes

$$R/2Ja(3\kappa/\pi)^{\frac{1}{2}} = t^{\frac{1}{2}},$$

which is the Plesset–Zwick approximation.

Equation (6) has been plotted in Fig. 17 for $C = 0, 100, 200$ and $400\ s^{-1}$. The trend indicated compares favorably with that exhibited by the data. The values of C for which the theory has been plotted correspond to velocities of the right order of magnitude. For example, for bubbles 13A and B (Fig. 10c), $C = 200\ s^{-1}$ corresponds to a velocity of 15 cm/s at 30 ms, not unreasonable for a bubble whose instantaneous radius is 0·075 cm. Notwithstanding the facts that (1) the theory is approximate and (2) the comparison hindered by lack of knowledge of $U = U(R)$, it is reasonable to conclude that the increased growth rates observed for the normal-g data may be attributed to the translational motion.

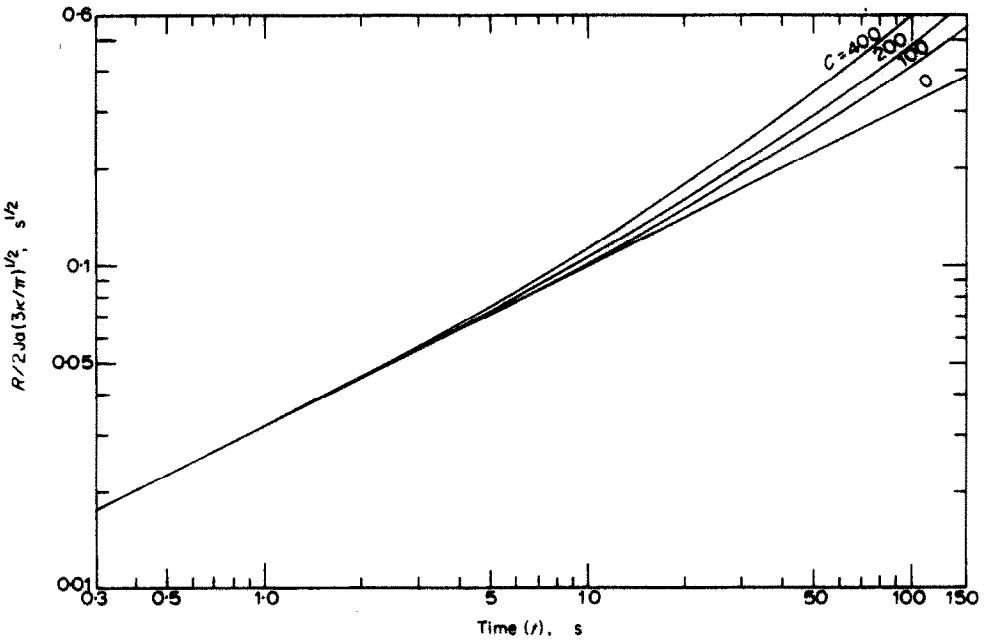

FIG. 17. Effect of bubble translational velocities based on approximate theory of Aleksandrov *et al.* [13].

PREVIOUSLY AVAILABLE DATA

The earliest data are those of Dergarabedian [8]. A comparison of most of this data to the Plesset–Zwick asymptotic solution was first presented in [3]. A direct comparison for one bubble was made in [8]. It is these comparisons which have been often cited as indicating excellent agreement. This data has been re-examined and compared to Scriven's result. Even allowing for the selection of an appropriate zero time it is difficult to obtain good agreement. Consider his Bubble 4 (Fig. 18a). Using the zero time from the original plots [8] results in the lowest set of data points. Adjusting the zero by 4 ms gives the uppermost set of data points which appears to show reasonable agreement until it is realized that, the first four data points now correspond to negative times and are *off* scale to the left. It is clear, however, from these first four data points that the bubble has already begun to grow. An intermediate zero time (t_0 = 2 ms) causes the data to cross over the theoretical curve at 1 ms. The data points to the right of 1 ms then fall only some 20 per cent below the theory, but two data points are still off scale to the left corresponding to negative times. Using t_0 = 1 ms, which would be the maximum allowable for Bubble 4 according to Dergarabedian, the data falls about 30 per cent below the theory and has a slope close to 2/3. It is interesting to note that this slope was used by Darby [25] to fit his data for bubbles nucleating from a horizontal surface while using an I.R. heating technique similar to Dergarabedian's. With t_0 = 1 ms, the data for Bubble 4 falls about midway between Scriven's result and Darby's fit to his own data. All of Dergarabedian's water data compares in a similar fashion to Scriven's prediction except for his Bubbles 1, 2 and 3 (ΔT = 1·4°C) which compare even less favorably* and his Bubbles 7, 8 and 9 (ΔT = 3·1°C) which give the best agreement. Data for Bubble 9 is plotted in Fig. 18b for three different zero times. Again note that for both t_0 = 1·5 and 3 ms several data points are off scale to the left.

* This is probably because of the relatively small superheat involved for these bubbles.

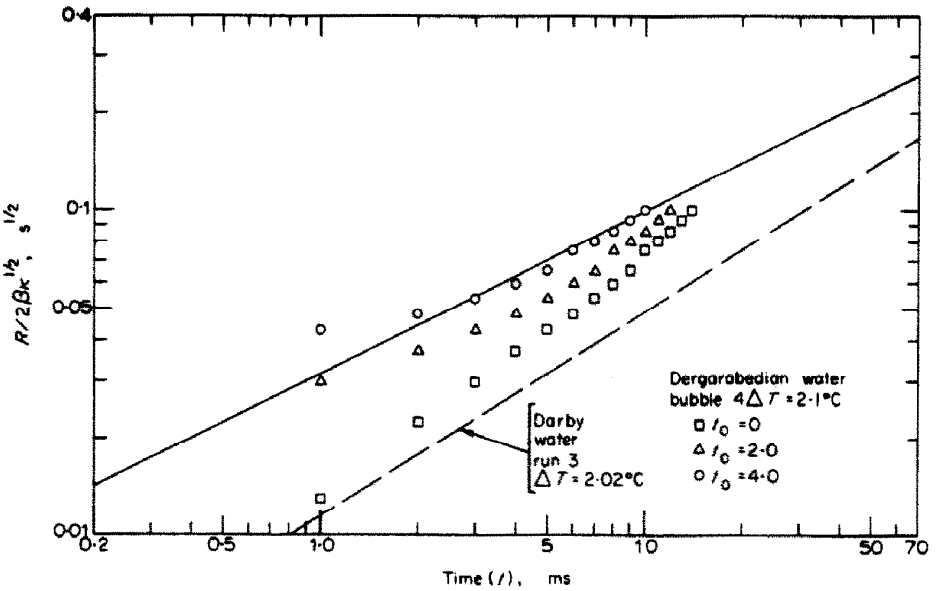

FIG. 18(a)

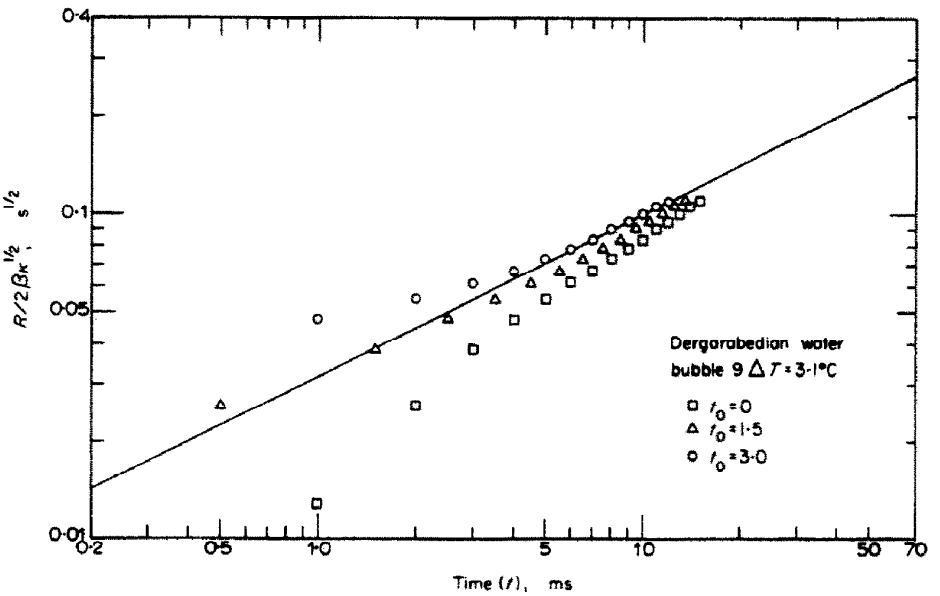

FIG. 18(b)

FIG. 18(a), (b). Example of comparison between Dergarabedian's water data and Scriven's theoretical result.

Comparison of Dergarabedian's organic liquid data [9] to Scriven's prediction shows much better agreement than his water data (Fig. 19).* An explanation for this is not clear, unless it is due to the sand and/or chalk dust sprinkled into the superheated water to cause nucleation. The bubbles then actually began growing on solid surfaces similar to the conditions in Darby's experiments, except the latter used a much larger surface. The similarity of slopes between the water data of Dergarabedian and Da.by when using, in both cases, a zero time obtained by direct extrapolation to zero has already been pointed out.

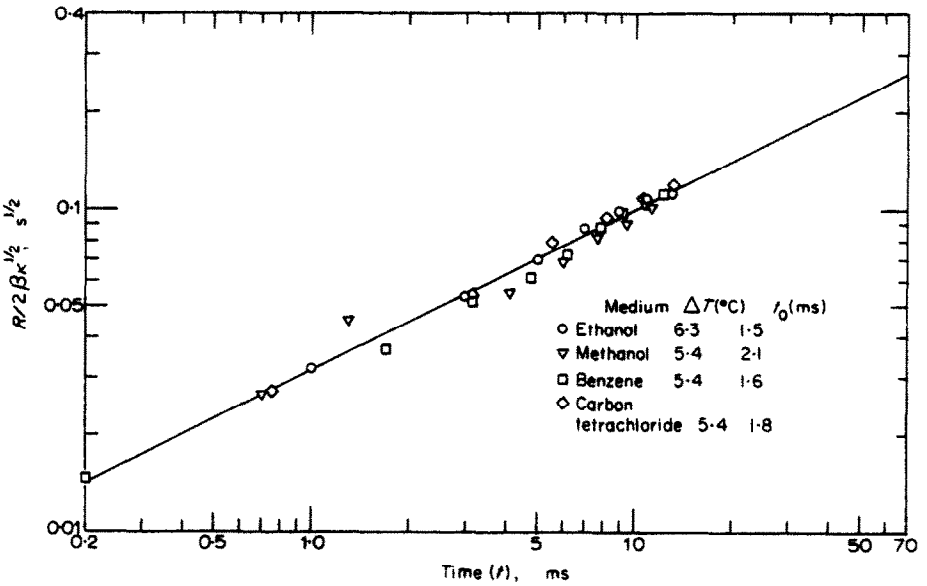

FIG. 19. Dergarabedian's organic liquid data compared with Scriven's theoretical result.

The data of Hooper and Abdelmessih [11] for a water vapor bubble growing at a constant superheat of 6·8°C and a pressure level of 1 atm. is in excellent agreement with Scriven's prediction for the relatively short observation time of 7 ms. However, for higher superheats the data falls increasingly below the theory. In [11] this is attributed to the neglect of liquid inertia effects, which also become increasingly important for higher superheats. However, Al-Jubouri [21] has shown that even for their maximum superheat of 38·8°C this explanation is incorrect. The explanation suggested by Kosky [14] is probably correct. Even though the pressurized system was suddenly released to an atmospheric environment, the transient system pressure was higher than one atmosphere thus resulting in a superheat substantially lower than quoted. However, contrary to Kosky's statement, reference [11] indicates that a pressure transducer was used for a simultaneous recording of the system pressure. To quote from [11]: "No bubble has been observed to begin with less than 4 ms delay beyond the termination of the decompression period." Apparently, they used a pressure pick-up (see their Fig. 2) but only to determine the initial decompression time (stated to be less than 5 ms) and its relation to the initiation of growth, and not to determine the magnitude of the decompression.

* It seems rather surprising, but to the authors' knowledge no detailed direct comparison of Dergarabedian's water or organic liquid data to equations (1) and (2) has previously appeared in the literature.

Kosky reported data for one water vapor bubble growing at an essentially constant superheat of 17°C obtained by decompression of the liquid system. The final pressure level was 0·488 atm. This data falls 20 per cent below Scriven's prediction but is just within the quoted experimental uncertainty.

Hewitt and Parker [12] reported data for nine bubbles in liquid nitrogen for constant superheats up to 4·5°C. Matching the first data point for each bubble exactly to the Plesset–Zwick theory, reasonable agreement was obtained. The matching procedure in effect fixed the zero time. Measured from this zero time the earliest data point for any bubble was observed at 18 ms. For the other eight bubbles the initial observation times ranged from 25 to 82 ms. The longest observation time *interval* was about 120 ms. However, the growth rates for these bubbles were such that the radii essentially only doubled over the observation interval.

Finally we note five data points for a propane bubble growing in a high pressure bubble chamber (17·1 atm.) at a superheat of 20·3°C reported by Aleksandrov *et al.* [13]. In [13] comparison was made to the approximate theory which results in equation (5) and reduces to the Plesset–Zwick theory when the translational velocity is zero. Fitting the theoretical curve to the data again fixed the zero time. The first data point fell at 18 ms and the final at 50 ms with satisfactory agreement. Again the bubble radius only doubled over the observed interval. It is interesting to note that the Jakob number for this bubble is only 2·4. At this value the Plesset–Zwick approximation falls some 20 per cent below the exact solution of Scriven. For this particular bubble agreement with Scriven's theory is almost as good as that using the Plesset–Zwick approximation, but with translational effects included, i.e. equation (5).

CONCLUDING REMARKS

New experimental data for growth rates of free vapor bubbles in liquids at essentially constant and uniform superheats has been presented. This includes measurements for 26 bubbles in three different liquids under normal -g conditions and measurements for nine bubbles in two different liquids under zero-g conditions. Initial observation times for individual bubbles were comparable to or smaller than those of previous investigations, while longer observation time intervals were achieved. Comparison of the normal to the zero-g data over these longer intervals clearly indicated the significance of the buoyant force.

The zero-g experimental conditions provided close approximation to the fundamental spherically symmetric theoretical model. Good agreement with Scriven's theoretical prediction based on such a model was obtained. Previous comparisons were limited to times less than those for which the translational effects become significant, since only normal-g conditions were used.

Semi-quantitative comparison between an approximate theory [13] and the normal-g data indicated that appropriate incorporation of translational effects into the theoretical model appears to account for the observed increase in growth rates. However, improvement in the detail of this comparison would be desirable from two standpoints; the refinement of the theory to make it more exact and accurate measurement of the bubble translational velocity relative to the liquid as a function of either bubble size or time.

Using a similar experimental technique as described herein, data for ethanol–water and isopropanol–water mixtures has also been obtained. This data provides direct experimental verification of Scriven's theory particularly with regard to the added effect of mass transport. Data has also been obtained for water containing a small quantity of a surface active agent. These results will be reported subsequently.

ACKNOWLEDGEMENTS

The authors would like to acknowledge the financial support of the National Science Foundation under NSF Grant GK-229. Partial support was also provided by an

Arizona State University Research Grant. One of the authors (CLH) received financial assistance from an Arizona State University Graduate Research Fellowship. Graduate students providing past assistance were Stewart Fischer and William Beck.

REFERENCES

1. G. Birkhoff, R. S. Margulies and W. A. Horning, Spherical bubble growth, *Phys. Fluids* **1**, 201–204 (1958).
2. L. E. Scriven, On the dynamics of phase growth, *Chem. Engng Sci.* **1**, 1–13 (1959).
3. M. S. Plesset and S. A. Zwick, The growth of vapor bubbles in superheated liquids, *J. Appl. Phys.* **25**, 493–500 (1954).
4. S. G. Bankoff, Diffusion controlled bubble growth, Review in *Advances in Chemical Engineering* (Edited by T. B. Drew *et al.*) pp. 14 and 36. Academic Press, New York (1966).
5. W. M. Rohsenow, Heat transfer with boiling. Review in *Modern Developments in Heat Transfer* (Edited by W. Ibele) p. 107. Academic Press, New York (1963).
6. L. S. Tong, *Boiling Heat Transfer and Two-Phase Flow*, p. 17. John Wiley, New York (1965).
7. J. W. Westwater, Things we don't know about boiling heat transfer, Review in *Theory and Fundamental Research in Heat Transfer* (Edited by J. A. Clark) p 68. Pergamon Press, New York (1963).
8. P. Dergarabedian, The rate of growth of vapor bubbles in superheated water, *J. Appl. Mech.* **20**, 537–545 (1953).
9. P. Dergarabedian, Observations on bubble growth in various superheated liquids, *J. Fluid Mech.* **9**, 39–48 (1960).
10. J. J. Kirkaldy, The time-dependent diffusion theory for condensation on spherical and plane surfaces, *Can. J. Phys.* **36**, 446–455 (1958).
11. F. C. Hooper and A. H. Abdelmessih, The flashing of liquids at higher superheats, *Proc. Third Int. Heat Transfer Conf.* **4**, 44–50 (1966).
12. H. C. Hewitt and J. D. Parker, Bubble growth and collapse in liquid nitrogen, *J. Heat Transfer*, **90**, 22–26 (1968).
13. Yu. A. Aleksandrov, G. S. Voronov, V. M. Gorbunkov, N. B. Delone and Yu. I. Nechayev *Bubble Chambers*, pp. 72–76. Translation by Scripta Technica, Indiana University Press, Bloomington and London (1967).
14. P. G. Kosky, Bubble growth measurements in uniformly superheated liquids, *Chem. Engng Sci* **23**, 695–706 (1968).
15. D. A. Labuntsov, B. A. Kol'chugin, V. S. Golovin, E. A. Zakharov and L. N. Vladimirova, Study of the growth of bubbles during boiling of saturated water within a wide range of pressures by means of high-speed moving pictures, *High Temperature*, vol. 2, pp. 404–409 (1964). English language translation by Consultants Bureau, New York, of *Teplofizika Vysokikh Temperatur*, Vol. 2, pp. 446–453 (1964).
16. J. M. Yatabe and J. W. Westwater, Bubble growth rates for ethanol-water and ethanol-isopropanol mixtures, A.I.Ch.E. Preprint 7, *8th Natn Heat Transfer Conf.*, A.I.Ch.E.–A.S.M.E., Los Angeles, California, (Aug. 8–11, 1965).
17. V. E. Schrock and J. P. Perrais, Dynamics of bubbles in a known temperature distribution, *Proc.* 1966 *Heat Transfer and Fluid Mech. Inst.*, pp. 122–147, Stanford University Press, Stanford, Calif. (1966).
18. R. Cole and H. L. Shulman, Bubble growth rates at high Jakob numbers, *Int. J. Heat Mass Transfer* **9**, 1377–1390 (1966).
19. W. Frost and C. J. Kippenhan, Bubble growth and heat transfer mechanisms in the forced convection boiling of water containing a surface active agent, *Int. J. Heat Mass Transfer* **10**, 931–949 (1967).
20. L. W. Florschuetz and B. T. Chao, On the mechanics of vapor bubble collapse, *J. Heat Transfer* **87**, 209–220 (1965).
21. A. Al-Jubouri, A generalized quantitative criterium to predict the rate controlling mechanism for growth of vapor bubbles in uniformly superheated liquids, Ph.D. dissertation, Arizona State University, Tempe, Arizona (1969).
22. S. A. Zwick and M. S. Plesset, On the dynamics of small vapor bubbles in liquids, *J. Math. Phys.* **33**, 308–330 (1955).
23. H. K. Forster and N. Zuber, Growth of a vapor bubble in a superheated liquid, *J. Appl. Phys.* **25**, 474–478 (1954).
24. L. A. Waldman and G. Houghton, Spherical phase growth in superheated liquids, *Chem. Engng Sci.* **20**, 625–636 (1965).
25. R. Darby, The dynamics of vapour bubbles in nucleate boiling, *Chem. Engng Sci.* **19**, 39–49 (1964).

Résumé— Des résultats expérimentaux nombreux sont présentés pour des vitesses de croissance de bulles de vapeur dans l'eau, l'éthanol et l'isopropanol à de faibles surchauffes uniformes allant jusqu'à 4,9°C. La vitesse de croissance de la phase se produisait dans le volume libre du liquide loin des surfaces solides et à un niveau nominal de pression de 1 atm. Des surchauffes essentiellement constantes et uniformes ont été obtenues par une technique de baisse de pression. Les temps initiaux d'observation pour la plupart des bulles se produisaient environ à 1 ms. Des temps finaux d'observation aussi importants que 450 ms ont été obtenus. La comparaison des résultats de croissance obtenus pour une pesanteur normale aux résultats à gravité nulle, à l'aide d'une petite tour à chute libre, montrent clairement à quel point les effets dus au mouvement de translation des bulles deviennent sensibles.

On a comparé de façon détaillée avec la solution exacte de Scriven pour une croissance de phase à symétrie sphérique et contrôlée par le transport de chaleur. Un bon accord est obtenu pour les résultats à gravité nulle pendant toute la durée d'observation, tandis que l'accord pour les résultats avec gravité

normale est satisfaisant jusqu'au moment où les effets de la force de flottaison deviennent sensibles. L'interprétation selon laquelle l'augmentation des vitesses de croissance observée à des instants postérieurs est due aux effets de translation des bulles est confirmée par une comparaison semi-quantitative avec une théorie approchée due à Aleksandrov *et al.*

On discute également les résultats expérimentaux antérieurs pour la croissance des bulles sous des conditions de surchauffe uniforme et essentiellement constante et leurs relations avec le travail actuel.

Zusammenfassung Es werden umfangreiche Messergebnisse für Wachstumsraten von Dampfblasen in Wasser, Äthanol und Iso-Propanol bei geringer, gleichmässiger Überhitzung bis 4,9°C vorgelegt. Die gemessene Wachstumsstufe lag im freien Flüssigkeitsraum entfernt von festen Oberflächen und bei einem Nominaldruckniveau von 1 atm. Gleichmässige, im wesentlichen konstante Überhitzung wurde durch ein Druckminderungs-Technik erzielt. Die meisten Blasen liessen sich nach etwa 1 ms zuerst beobachten. Endbeobachtungszeiten von 450 ms wurden erreicht. Ein Vergleich der Wachstumsdaten bei normaler Erdbeschleunigung mit den bei Gravitation Null mittels eineskleinen Fallgestells gemessenen, zeigt klar den Punkt, an dem der Einfluss der Blasenfortbewegung wesentlich wird.

Ein detaillierter Vergleich mit Scrivens exakter Lösung für kugelsymmetrisches, wärmeübergangsabhängiges Phasenwachstum wurde durchgeführt. Gute Übereinstimmung wurde für die Null-g Werte über den ganzen Beobachtungszeitraum erreicht, während die Übereinstimmung für die Normal-g Werte nur bis zu dem Zeitpunkt reicht, bei dem der Einfluss der Auftriebskraft wesentlich wird. Eine Interpretation in dem Sinne, dass die angestiegenen Wachstumsraten, die zu späterer Zeit beobachtet wurden, von dem Einfluss des Blasenfortschreitens abhängig sind, wurde durch einen halbquantitativen Vergleich mit einer Näherungstheorie von Aleksandrov und anderen unterstützt.

Frühere experimentelle Ergebnisse für das Blasenwachstum unter gleichmässigen, im wesentlichen konstanten Überhitzungsbedingungen und ihre Beziehung zu der vorliegenden Arbeit wurden auch diskutiert.

Аннотация—Представлены многочисленные экспериментальные данные по исследованию скорости роста пузырьков пара в воде, спирте и изопропаноле при небольшом однородном перегреве до 4,9°C. Измеряемый рост фазы происходил в свободном объеме жидкости в стороне от твердых поверхностей и при номинальном уровне давления в 1 атм. Однородные в основном постоянные перегревы достигались снижением давления. Начальные моменты наблюдения для большинства пузырьков составляили около 1 мсек. Конечные моменты наблюдениядо 450 мсек. Путем сравнения данных о росте пузырьков, полученных на небольшой капельной башне при обычной силе тяжести, с данными, полученными при нулевой силе тяжести, точно определена точка, при которой становятся значительными эффекты, возникающие из-за поступательного движения.

Проведено подробное сравнение с точным решением Скривена для сферически симметричного контролируемого теплообменом роста фазы. Для всего времени наблюдения получено хорошее согласование данных при нулевой силе тяжести является удовлетворительным до того момента, пока не становятся знаутельными эффекты плавучести. Это объяснение, что наблюдаемые позже увеличенные скорости роста обусловлены поступательными эффектами пузырьков, подтверхдается полуколичественным сравнением с приближенной теорией Александрова и др.

Обсуждаются экспериментальные данные о росте пузырьков при однородных в основном постоянных условиях перегрева и их связь с данной работой.